ELSEVIER

PII: S0032-3861(96)00666-0

Polymer Vol. 38 No. 7, pp. 1639–1646, 1997

0032-3861/97/$17.00+0.00

A parametric study of microencapsulation approach to the preparation of polystyrene shells

Emmanuel L. Alfonso*†‡, Shaw H. Chen*†‡§, Mark D. Wittman‡, Semyon Papernov‡ and David Harding‡

**Materials Science Program, †Department of Chemical Engineering, and ‡Laboratory for Laser Energetics, Center for Optoelectronics and Imaging, University of Rochester, 240 East River Road, Rochester, NY 14623-1212, USA*

(Received 18 December 1995; revised 15 June 1996)

Spherical polystyrene shells for laser fusion experiments were made in a density-matched microencapsulation approach. The yield, diameter, wall thickness, vacuole content, and surface finish were determined for different polystyrene concentrations varied from 5 to 13 wt% in an equivolume mixture of toluene and 1,2-dichloroethane, and an internal water phase containing surfactants, Tween 40 and Brij 30, at concentrations of 0.05 and 0.1 wt%, respectively. The main observations are: (1) The yield of shells is improved with added surfactants, and the effect is more pronounced at a higher polymer concentration; (2) The outer shell diameter increased with added surfactants at a constant polymer concentration. This is attributed to larger droplets being more stable in the first stage of the fabrication process; (3) Thicker shell walls are achieved with higher polymer concentrations; (4) The outer shell diameter increased with increasing polymer concentration regardless of added surfactants. This is attributed to a thicker wall providing greater mechanical stability; (5) The number of vacuoles over the cross-sectional area of the wall increases with increasing polymer concentration and with the addition of surfactants; and (6) The shells possess a smooth surface with a root-mean-square surface roughness less than 25 nm over a 30 μm × 30 μm area, and a sphericity greater than 99.6%.

INTRODUCTION

The term *nano-* or *microsphere* refers to a hollow or solid spherical structure that ranges in size from tens of nanometres to a few millimetres. Four microsphere fabrication methods exist[1]: (1) sacrificial cores; (2) nozzle–reactor systems; (3) emulsion/phase separation techniques; and (4) spheres by mechanical attrition. Manufacture with sacrificial cores requires coating the material of interest onto a core, which is then dissolved in a solvent or vaporized[2]. The remaining coating material forms a hollow microsphere. Common forms of the nozzle-reactor system include spray drying[3] or pyrolysis[4]. These methods are appropriate when strict geometric specifications are not critical. Microspheres with exacting specifications on sphericity, wall thickness, and diameter, may be created with carefully designed nozzle systems which create individual liquid droplets[5]. The emulsion/phase separation technique relies on surface tension and immiscibility of the two phases[6,7]. The dispersed phase forms droplets in a liquid matrix, then various chemical and/or physical techniques are used to process the liquid droplets into rigid spheres of interest. Finally, spheres made by mechanical attrition can be produced by placing roughly spherical material into matching grooves in two opposing plates[8,9]. Rotating one of the plates grinds the sphere to an acceptable sphericity.

The potential applications of solid and hollow spheres are quite diverse[10]. Hemoglobin microbubbles, formed by crosslinking cysteine residues of serum albumin protein around a gas bubble or liquid droplet, are being created as a possible blood substitute[11]. An emulsion method is used to create doped porous glass microspheres for use in fibre optic sensors[12]. Dispersed spheres of conductive indium oxide (In_2O_3) are blended into a polymer matrix to form antistatic and thermal barriers for spacecrafts[13]. Finally, shells are used as fuel containers in inertial confinement fusion (ICF) experiments[14].

Plastic shells are being explored in this study as a fuel containers for laser fusion. Methods to make shells reported in the literature include the droplet generator[15,16], sol gel processing[17,18], and interfacial polycondensation[19] methods. Drawbacks of these existing methods include low sphericity, nonuniformity of shells, and low overall yields. We have produced hollow polystyrene shells in a density-matched water/oil/water fluid system, called *microencapsulation*. This study investigates the manner in which system parameters, such as addition of surfactants, viscosity, and polymer concentration, affect the shell's outer diameter. We have also investigated the effects of these parameters on shell quality, wall thickness, and overall yield. Previous work on this method has not attempted to quantify effects of these system parameters.

§ To whom correspondence should be addressed

EXPERIMENTAL

Materials

Polystyrene ($\bar{M}_w = 90\,000$ g mol^{-1}; $\bar{M}_w/\bar{M}_n \leq 1.04$; Pressure Chemical Company; or $\bar{M}_w = 150\,000$ g mol^{-1}; $\bar{M}_w/\bar{M}_n = 1.4$; Scientific Polymer Products, Inc.), polyvinyl alcohol ($\bar{M}_n = 25\,000$; $\bar{M}_w/\bar{M}_n = 2$; 88 mol% hydrolysed; Polysciences, Inc.), reagent-grade solvents 1,2-dichloroethane and toluene (both from J. T. Baker, Inc.) and ethanol (EM Science), surfactants Tween® 40 (polyoxyethylene (20) sorbitan monopalmitate) and Brij® 30 (polyoxyethylene (4) lauryl ether) (both from Aldrich Chemical Company) were all used as received without further purification. Distilled, deionized water was used in the preparation of all aqueous phases.

Fabrication procedure

The microencapsulation method described below is a variation of the methods developed by Takagi *et al.*[20] and Kubo *et al.*[21], and the process is as depicted in *Figure 1*. Polystyrene (PS) was dissolved in an equivolume mixture of 1,2-dichloroethane and toluene to make the oil (*O*) phase with a density of 1.08 g mL^{-1}. The amount of PS in the mixture varied from 5 to 13 wt%, and its molecular weight was 90 000 g mol^{-1}, unless stated otherwise. The *O* phase was filtered to remove particulates larger than 0.2 μm. The internal water phase, W_1, was poured into the *O* phase stirred at 400 rpm to form an emulsion of water droplets in oil. W_1 was distilled water which, in some cases, contained surfactants. An aqueous solution of 1.4 wt% polyvinyl alcohol (PVA) was used as the continuous water phase, W_2. The W_1/O emulsion was quickly poured into a beaker containing the heated, stirred W_2 phase to form a $W_1/O/W_2$ emulsion. The stirring provided gentle suspension of the droplets during the heating process.

The $W_1/O/W_2$ emulsion was heated in a water bath at 76°C until all the solvents were removed from the *O* phase (4 h). The remaining products are solid wall PS shells containing water (W_1) on the inside. The shells were washed gently with distilled water to remove residual PVA from their outer surfaces. The shells were then placed in ethanol to replace the internal W_1. This water displacement procedure was performed in two steps to minimize shell breakage caused by the volume change due to counter diffusion of ethanol and water through the wall. The shells were dried under gentle heating (40°C) at atmospheric pressure for at least two days. Finally, the shells were dried overnight *in vacuo* to remove residual solvents.

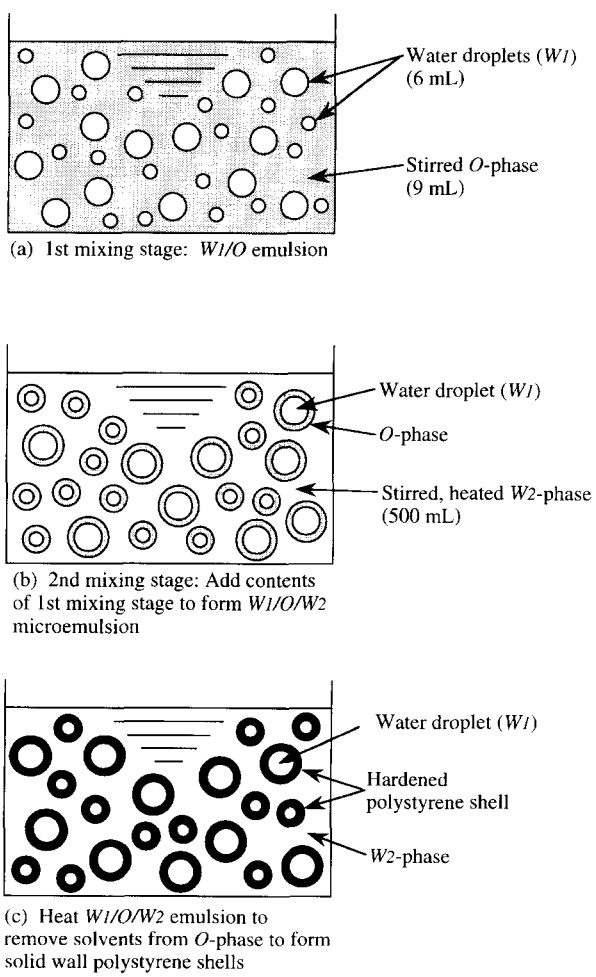

Figure 1 Schematic of microencapsulation procedure: (a) first mixing stage; (b) second mixing stage; (c) solvent removal/shell hardening in second mixing stage

Characterization

The outer diameter of a shell was determined with an Nikon Optiphot optical microscope equipped with an HMOS™ Micro-Measure digital scaler.

For sphericity measurements, the outer diameter was measured at a higher magnification to the nearest 0.1 μm. The shell placed on the vacuum chuck was rotated about its axis 30°, and the measurement was repeated. Six measurements were taken while rotating about one axis. The shell was then picked up by a vacuum chuck placed perpendicular to the first orientation, and the process was repeated for six more measurements. The sphericity, *s*, of a shell is defined as

$$s = [1 - (D_{max} - D_{avg})/D_{avg}] \times 100\%$$

where D_{max} is the maximum value of the outer diameter, and D_{avg} is the average outer diameter from the 12 measurements.

Scanning electron microscopy (SEM) (Cambridge S200) was used to observe inner and outer shell surface quality up to 20 000 × magnification. Several shells from each batch were frozen with liquid nitrogen, then pierced or cracked to view the inner surfaces and wall cross section. A typical shell and its outside surface are as shown in *Figures 2* and *3*. The wall thickness was determined directly from the SEM micrographs, as shown in *Figure 4*. Several shells produced under each experimental condition were measured to determine the average wall thickness.

The interfacial tension of the solutions was measured with a duNouy tensiometer (CSC Scientific Company, Inc.; Model 70545). The solutions were filtered to remove particulates, and the measurements were taken in accordance with the specifications of ASTM Standard Method D1331-89 for surfactant solutions.

The viscosity of the PS solution was measured with a cone-and-plate viscometer (Brookfield Engineering Laboratories, Inc.; Model RVDV II +), equipped with a 2.4 cm cone which made a 0.8° angle with the plate. Each solution was quickly enclosed in the sample cup to prevent solvent evaporation. The reported values of

T1277

Figure 2 SEM micrograph: A typical polystyrene shell. The shell had been punctured to view the inner surface and wall cross-section

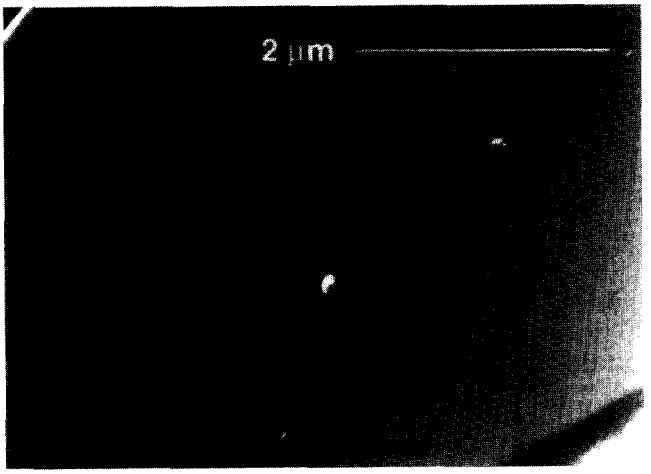

T1276

Figure 3 SEM micrograph: Outer surface of a polystyrene shell

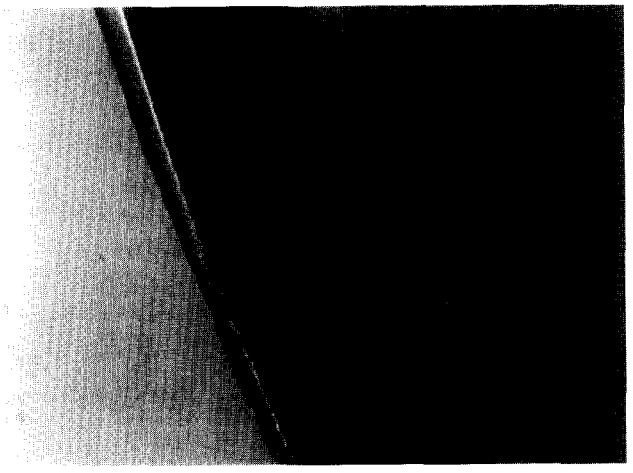

T1273

Figure 4 SEM micrograph: Polystyrene shell wall cross section. No vacuoles are present in the shell wall

solution viscosity are those at zero shear rate and were constant over nearly two decades of shear rate.

The number of vacuoles on a shell was determined with an optical microscope. Vacuoles appear as dark spots in the transparent shell wall. A square grid (23.9 μm × 23.9 μm) was projected onto the shell surface and the number of vacuoles contained in the grid were counted. The number of vacuoles in three size ranges ($\nu \geqslant 5\,\mu$m, $5 > \nu \geqslant 3\,\mu$m, and $\nu < 3\,\mu$m) was recorded, where ν is the diameter of the vacuole. The grid was moved after each measurement and the procedure was repeated 10 times per shell. These measurements were taken on shells with outer diameter greater than 700 μm.

Surface microscopy was carried out on a Nanoscope-III (Digital Instruments, Inc.) Atomic Force Microscope (AFM) to determine surface roughness. On smooth areas with peak-to-valley variations less than 500 nm and lacking steep structural features, standard silicon nitride (Si_3N_4) probes proved adequate. A challenge did arise from the 'stickiness' of the probes to the sample. Adjustments to the microscope feedback loop and reducing the scanning speed were successful countermeasures in this case. Microscope resolution was limited by residual system vibration noise that remained after isolation of the entire AFM/optical microscope monitor assembly on commercial vibration-isolation mounts. Cleaved mica surfaces were readily imaged at atomic scale resolution in this microscope mounting configuration. Force minimization precautions were always taken in order to prevent modification of the sample by the probe.

RESULTS AND DISCUSSION

Overall shell yield

As the 1,2-dichloroethane/toluene mixture is removed by heating and subsequent evaporation from the O phase, the PS forms a hardened, solid-wall-shell. After thorough washing with water, the shells are immersed in ethanol. As ethanol diffuses through the shell wall and replaces W_1, a small air bubble forms at the centre. This process occurs for shells with crack-free, unbroken walls. The air bubble causes the unbroken shells to float in the ethanol bath, providing a convenient way to separate intact shells from cracked or broken ones. The floating shells are the ones selected to be dried for extensive characterization.

The success of a polymer shell fabrication process depends on the number of high quality shells produced by the method. Successful runs using the present method may produce several hundred to a few thousand unbroken shells per gram of PS. High quality targets must be vacuole-free, unbroken shells with very little or no surface debris, a uniform wall thickness, and a high degree of sphericity. What we report as the overall shell yield does not take into account the 'target quality' of the shell. In the present work, the yield of shells was defined as the percentage of the mass of unbroken shells compared to the initial mass of PS in the O phase. As shown in *Table 1*, the yield of shells produced with 0.05 wt% Tween 40 in the W_1 phase was found to be consistently greater than those prepared in its absence.

The presence of a surfactant in the W_1 phase lowers the interfacial tension between the W_1/O phases. In a run performed with a polystyrene concentration, C, of

Table 1 Overall shell yield as a function of added surfactants

Polystyrene concentration (wt%)	Overall yield[a] (wt%) Tween 40 (0.05 wt%)	Brij 30 (0.1 wt%)	No added surfactants
5	3.4	—	2.3
7	14	6.2	3.4
10	34	8.5	11
13	38	—	6.4

[a] Overall yield is defined as the weight of polystyrene forming unbroken shells after thorough drying divided by the weight charged in the first mixing stage

7 wt%, the interfacial tension ranged from 29 dynes cm^{-1} for no surfactant, to 12 dynes cm^{-1} for 0.05 wt% Tween 40 in W_1. The interfacial tension data are as presented in *Table 2*. We believe the benefits of surfactant are two-fold. The surfactant aids in the droplet breakup and dispersion in the W_1/O emulsion by lowering interfacial tension. Thus, more droplets are created in the stirred W_1/O, which leads to more shells. Secondly, surfactant prevents the coalescence of resultant droplets, increasing their chance for survival in forming shells.

Shells were also produced with Brij 30 (0.1 wt%) as the surfactant in the W_1 phase. The interfacial tension at the W_1/O boundary was 21 dynes cm^{-1}. It was found that overall shell yields are comparable to those with pure water as the internal phase. The shells produced under these conditions also appeared cloudy, and few shells displayed self-interference patterns, which suggest that these shells have non-uniform wall thickness and/or sphericity.

Outer diameter and wall thickness

The outer diameters of individual dried shells were measured to the nearest 1 μm in determination of the average diameter. At least 150 unbroken shells were included in the calculation of number average outer diameter, D, for each experimental run. The observed D values for two to three experimental runs were employed to calculate the mean outer diameter, $\langle D \rangle$, as reported along with standard deviation in *Table 3*. Similarly, the mean wall thickness, $\langle \delta \rangle$, was calculated from number average thickness determined for two to three experimental runs under a given set of conditions. The mean inner diameter, $\langle d \rangle$, was then calculated using $\langle d \rangle = \langle D \rangle - 2\langle \delta \rangle$. The resultant values of $\langle \delta \rangle$ and $\langle d \rangle$, are also included in *Table 3*. Note that both $\langle D \rangle$ and $\langle d \rangle$ increase with added surfactants at a given value of C and with an

Table 2 Interfacial tension and zero-shear viscosity of oil phase

Polystyrene concentration (wt%)	Interfacial tension (dynes cm^{-1}) Tween 40 (0.05 wt%)	Brij 30 (0.1 wt%)	No added surfactants	Viscosity of oil phase (cP)
5	12.9 ± 0.6	—	31 ± 1	4.1
7	11.7 ± 0.5	20.8 ± 0.9	29.4 ± 0.9	6.8
10	9.5 ± 0.6	16.6 ± 0.7	28 ± 1	13.6
13	9.1 ± 0.8	—	28 ± 1	25.2

Table 3 Experimentally measured outer diameter, $\langle D \rangle$, wall thickness, $\langle \delta \rangle$, and inner diameter, $\langle d \rangle$, calculated based on $\langle d \rangle = \langle D \rangle - 2\langle \delta \rangle$

Polystyrene concentration (wt%)	Mean outer diameter, $\langle D \rangle$ [μm] Tween 40 (0.05 wt%)	Brij 30 (0.1 wt%)	No added surfactants
5	603 ± 33	—	552 ± 25
7	675 ± 26	621 ± 9	585 ± 8
10	720 ± 32	688	629 ± 17
13	785 ± 9	—	702 ± 20
Polystyrene concentration (wt%)	Mean wall thickness, $\langle \delta \rangle$ (μm) Tween 40 (0.05 wt%)	Brij 30 (0.1 wt%)	No added surfactants
5	8 ± 2	—	7 ± 2
7	9 ± 2	10 ± 2	10 ± 2
10	13 ± 4	16 ± 6	10 ± 4
13	20 ± 6	—	22 ± 7
Polystyrene concentration (wt%)	Mean inner diameter, $\langle d \rangle$ (μm) Tween 40 (0.05 wt%)	Brij 30 (0.1 wt%)	No added surfactants
5	587	—	538
7	657	601	565
10	694	656	609
13	745	—	658

Table 4 Aspect ratio, $A = \langle D \rangle / 2\langle \delta \rangle$, calculated with values of $\langle D \rangle$ and $\langle \delta \rangle$ reported in *Table 3*

Polystyrene concentration (wt%)	Tween 40 (0.05 wt%)	Aspect ratio, A Brij 30 (0.1 wt%)	No added surfactants
5	38	—	39
7	38	31	29
10	28	22	31
13	20	—	16

increasing C for a given W_1 phase composition. In contrast, while an increasing value of C appears to contribute to a thicker $\langle \delta \rangle$, its value remains roughly unaffected by added surfactants.

The shells produced with Brij 30 (0.1 wt%) in the internal water phase had average outer diameters between the pure water and Tween 40 cases under otherwise identical experimental conditions. Similarly, the interfacial tension between the W_1/O phases containing 0.1 wt% Brij 30 was measured to be 21 dynes cm^{-1}, compared to 12 and 29 dynes cm^{-1} for the Tween 40 (0.05 wt%) and pure water cases, respectively. The effect of interfacial tension on shell size appears to be counter intuitive. At the same mixing power input, a lower interfacial tension should result in more interfacial area and thus lead to smaller droplets. The presence of a surfactant facilitates droplet breakup. It also allows stabilization of the larger droplets by inhibiting their coalescence. In the absence of surfactants, the breakup of W_1 in the O phase was not as favourable, and the resultant larger droplets were unstable and coalesced readily without contributing to formed shells. This is also apparent in the diminished overall shell yield as listed in *Table 1*.

The average droplet size in an emulsion may also depend on the viscosities of the dispersed and continuous phases. In the first mixing stage as depicted in *Figure 1a*, these phases correspond to W_1 and O, respectively. Although the W_1 viscosity is the same in each case, the O phase viscosity increases with C, as reported in *Table 2*. In all cases, the stirring speed while mixing W_1 and O remained constant. If the shear rate of the fluid remained constant, then the stress caused by the fluid is proportional to the viscosity. According to the literature on droplet size in liquid–liquid dispersions[22], it appears that the greater shearing force of a higher viscosity liquid against the W_1 phase facilitates dispersion, and would result in smaller W_1 droplets. A relevant experiment was

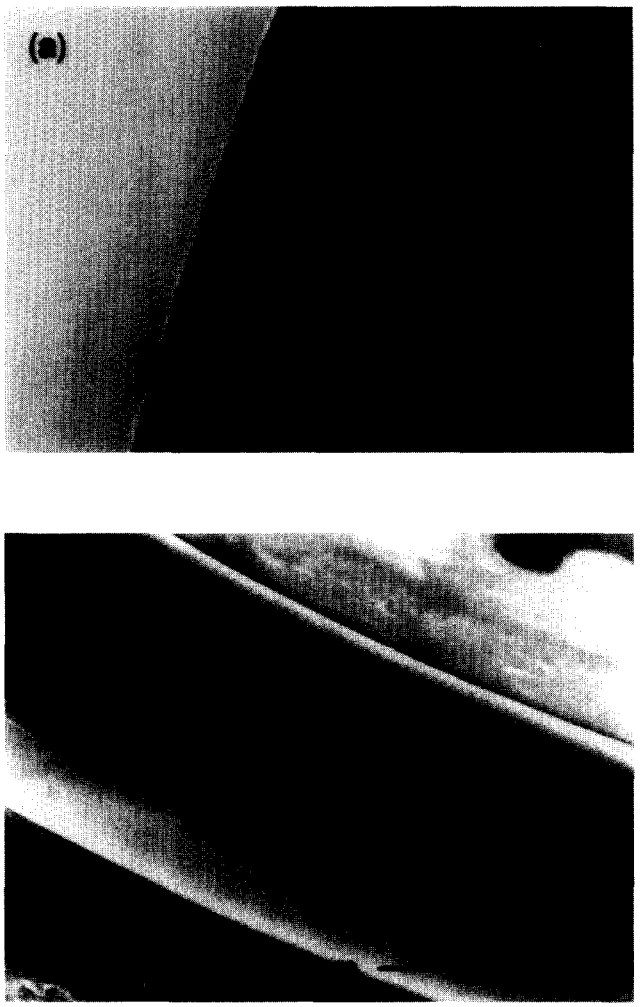

T1275

Figure 5 SEM micrographs: Shell wall cross sections. Vacuoles of various sizes appear throughout the wall

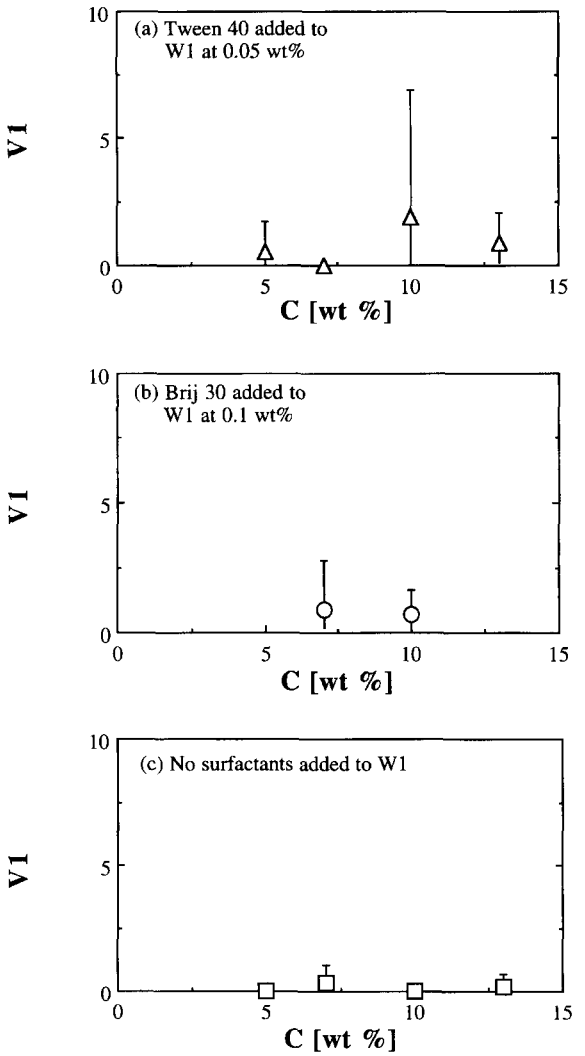

Figure 6 V_1: Number of vacuoles per 10 000 μm^2 with diameter $\nu \geq 5\,\mu m$ for cases of W_1 containing (a) Tween 40 at 0.5 wt%, (b) Brij 30 at 0.1 wt%, and (c) no surfactant. The shells with D greater than 700 μm were employed for this determination

performed to explore this hypothesis for the present case of microencapsulation. To increase the viscosity without increasing the amount of polymer, a 150 000 g mol^{-1} molecular weight PS sample was used to make a 7 wt% *O* phase to compare with the similar 90 000 g mol^{-1} case. The viscosity was found to be 67% greater for the higher molecular weight polymer solution. Shells were fabricated under otherwise identical conditions. Indeed, the average outer diameter of the shells made with the higher molecular weight sample was 600 μm, lower than $\langle D \rangle$ of 675 μm for the lower molecular weight case. Thus, $\langle D \rangle$ decreases with an increase in the viscosity of the *O* phase, as expected.

Therefore, the increasing trend in $\langle D \rangle$ with increasing *C* cannot be accounted for by the effect of *O* phase viscosity on W_1 droplet diameter. We rationalise the observed correlation between $\langle D \rangle$ and *C* in terms of mechanical stability of microencapsulation. To place this argument on a semi-quantitative basis, the aspect ratio, as defined by $A \equiv \langle D \rangle / 2\langle \delta \rangle$, was calculated, and the results are presented in *Table 4*. Note the decreasing *A* value at an increasing value of *C*, suggesting that a thicker wall is required for a larger shell produced at a higher polymer concentration to survive the shell fabrication process. At a lower *C*, the resultant thinner wall is not sufficient to prevent larger shells from cracking or collapsing. This interpretation is applicable to all cases, i.e. both in the absence and presence of surfactants.

Shell wall quality

As the W_1 phase is introduced to the stirred *O* phase, water diffuses rapidly into the organic phase until saturation. When heating begins and the solvents from the *O* phase are being removed, the polymer concentration in the shell increases. As a consequence, the viscosity of the *O* phase increases, thereby slowing diffusion processes. Driving force for the removal of water from the shell wall is never high because the shell is surrounded by water on both inner and outer surfaces. The water in the *O* phase shell reaches supersaturation as the organic solvent is continually removed, resulting in micrometre-sized droplets within the shell wall[23]. Upon complete drying, the water leaves a bubble, or vacuole, in the shell wall.

Typically, PS has been found to be capable of forming high quality shells. Relatively vacuole-free walls have been reported for *C* ranging from 3 to 5 wt%[20].

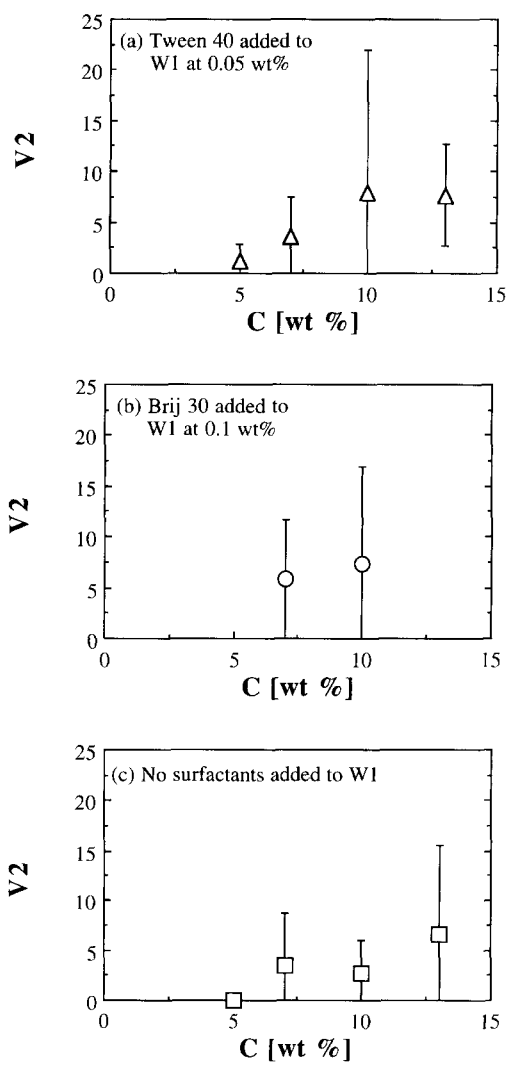

Figure 7 V_2: Number of vacuoles per 10 000 μm^2 with diameter $5 > \nu > 3$ μm for cases of W_1 containing (a) Tween 40 at 0.5 wt%, (b) Brij 30 at 0.1 wt%, and (c) no surfactant. The shells with *D* greater than 700 μm were employed for this determination

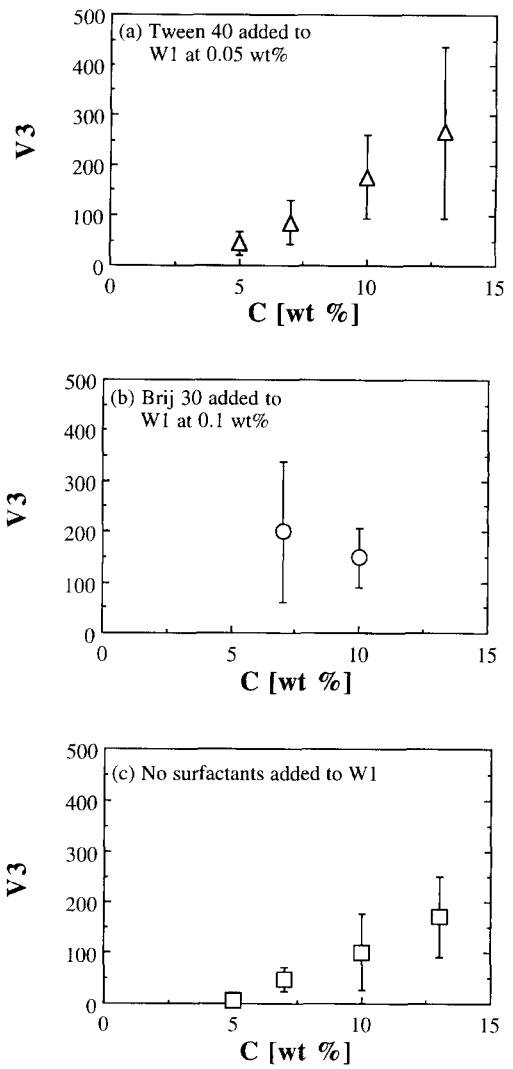

Figure 8 V_3: Number of vacuoles per 10 000 μm^2 with diameter $3\ \mu m > \nu$ for cases of W_1 containing (a) Tween 40 at 0.5 wt%, (b) Brij 30 at 0.1 wt%, and (c) no surfactant. The shells with *D* greater than 700 μm were employed for this determination

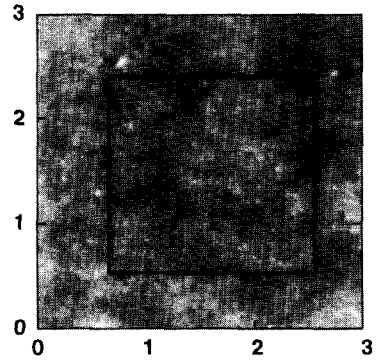

Roughness analysis

Image statistics

Z range	10.002 nm
Mean	0.00008 nm
rms (Rq)	0.830 nm
Mean roughness (Ra)	0.655 nm
Max height (R_{max})	10.002 nm

Box statistics

Z range	7.654 nm
Mean	0.010 nm
rms (Rq)	0.799 nm
Mean roughness (Ra)	0.625 nm
Max height (R_{max})	7.659 nm
Box x dimension	1.908 μm
Box y dimension	1.879 μm

Figure 9 AFM surface plot: Typical scan for small area (3 μm × 3 μm)

Examples of shell walls with vacuoles are given in *Figures 5a* and *b*, while vacuole-free walls are shown in *Figure 4*. We have defined a method of reporting the number of vacuoles in the shell wall by counting the vacuoles that appear in a square grid projected onto the shell surface. The number density of vacuoles will be reported as follows: V_1 = number of vacuoles with $\nu \geqslant 5\,\mu$m per 10 000 μm^2; V = number of vacuoles with $5 > \nu \geqslant 3\,\mu$m per 10 000 μm^2; and V_3 = number of vacuoles with $\nu < 3\,\mu$m per 10 000 μm^2, where ν is the diameter of the vacuole. These data are displayed in *Figures 6–8*, for shells with an outer diameter greater than 700 μm. We observed a low vacuole density at C of 5 and 7 wt% as well. For a 5 wt% PS solution and pure water W_1, we found the value V_3 to be about 5, with many shells virtually vacuole-free. Larger vacuoles (types V_1 and V_2) were essentially nonexistent. At higher values of C, the number of vacuoles of all types increases. This is probably due to the higher viscosity of the high concentration conditions, which inhibits water diffusion and removal. An experimental run using 15 000 g mol^{-1} molecular weight PS, giving a 67% increase in viscosity, was performed to explore this hypothesis. The initial concentration and processing conditions were kept similar to other experiments at 7 wt%. The shells produced with the higher molecular weight polymer had a marked increase in vacuole density. For example, with a 7 wt% solution of 90 000 g mol^{-1} PS using Tween 40 in the W_1 phase, V_1, V_2, and V_3 were found to be 0, 3.6, and 86, respectively. Under identical conditions with the 150 000 g mol^{-1} polymer, V_1, V_2, and V_3 were 1.8, 7.0, and 310, respectively.

It was also found that a surfactant-free W_1 phase yields shells with less vacuoles. For cases of 90 000 g mol^{-1} PS concentrations, 7, 10, and 13 wt%, the number of small vacuoles (V_3) is roughly 75% greater in the Tween 40 cases. For 5 wt% PS, the increase in V_3 is almost 750%. The same trend can be seen for larger vacuoles V_1 and V_2, as well. We believe the reason for the increase in vacuoles is due to the increased droplet breakup in the W_1/O mixing stage. The surfactant allows the W_1 to be broken into micrometre-sized droplets which are mixed into the O phase. When the solvents are removed from the O phase in the heating stage, the very small water droplets remain trapped in the viscous solution and become incorporated in the solid wall of the PS shell.

Besides the concern with the presence of vacuoles within the shell wall, surface finish is of primary importance to the development of a successful ICF technology. From SEM micrographs such as *Figure 3*, it was found that outer shell surfaces are typically smooth with very little debris. With SEM we were able to qualitatively observe the surface quality over a large area of the shell. Many precautions are taken to prevent particulates from adhering to the surfaces during processing, drying handling, and storage, but some defects may be unavoidable during these processes. AFM was used to quantitatively determine the surface roughness of the targets. Scans of the target surface suffered from some fundamental difficulties. Large 'bumps' on the surface may be due to dust or debris settling on the shell surface. Scans over an area greater than 30 μm × 30 μm could not be performed due to the height variations caused by curvature of the spherical surface. The saddled corners of the scan contributed significantly to the calculation of roughness. This effect was reduced by selecting shells with an outer diameter greater than 1000 μm for all AFM scans. Also, standard flattening and plane-fitting procedures incorporated in the software partially corrected this problem in smaller scans. The root-mean-square (r.m.s.) roughness value of 9.6 nm measured on a smaller area of the scan containing a 'flatter' region was less than the r.m.s. value of 20 nm over the entire 30 μm × 30 μm scanned area. Nevertheless, scans of 3 μm × 3 μm areas yield r.m.s. values of approximately 1 nm for surfaces of shells made at all values of C and internal water composition; a typical AFM surface plot is shown in *Figure 9*. As the size of the scan increases, the roughness value also increases because of the aforementioned problems of surface debris and curvature. The r.m.s. value, however, was never greater than 25 nm in scans over an area of up to 30 μm × 30 μm, which meets current surface finish requirements. Thus, it appears that the microencapsulation method is promising for producing shells with low r.m.s. values.

For effective compression of the target, it is required that the target is perfectly spherical. Earlier problems of nonsphericity were corrected by the technique of density-matching, where the densities of the O is adjusted to be nearly equal to that of W_1. This minimizes the effect of gravity which causes the walls of the shell to sag during the solvent removal stage and leads to

nonuniformity. In the present work, shells were produced having an average sphericity at least 99.6%, comparable to existing literature[20].

CONCLUSION

Polystyrene shells for use as ICF targets were produced following a density-matched water/oil/water ($W_1/O/W_2$) microencapsulation method. The overall yield of shells was found to increase with the addition of a surfactant to the internal water phase. The effect of added surfactants on improving overall yield is much greater at higher polymer concentrations, with yields close to 40%.

All methods produced some shells with an outer diameter over 1 mm. The increasing trend in $\langle D \rangle$ with added surfactants was attributed to the stabilization of larger droplets of W_1 in O, and the increasing trend in $\langle D \rangle$ with C to the improved mechanical stability contributed by a thicker shell wall. Whereas there was no noticeable effect of the composition of the internal phase on $\langle \delta \rangle$, its value was found to increase at an increasing value of C.

Many shells produced with 5 and 7 wt% PS solutions had relatively vacuole-free walls. Vacuoles were more problematic for C greater than 10 wt%. Shells made with surfactants in W_1 consistently had more vacuoles than those made with pure water in the internal phase. Sphericity and surface finish of the shells meet current requirements.

ACKNOWLEDGEMENTS

We would like to express our gratitude to B. McIntyre of the Institute of Optics, University of Rochester for his assistance with SEM. We would like to thank S. Noyes of the Laboratory for Laser Energetics, University of Rochester and M. Takagi of the Institute of Laser Engineering, Osaka University for their technical assistance with shell fabrication. This work was supported by the U.S. Department of Energy Office of Inertial Confinement Fusion under Cooperative Agreement No. DE-FC03-92SF19460, the University of Rochester, and the New York State Energy Research and Development Authority. The support of DOE does not constitute an endorsement by DOE of the views expressed in this article.

REFERENCES

1 Wilcox, D. L. and Berg, M. in 'Hollow and Solid Spheres and Microspheres: Science and Technology Associated With Their Fabrication and Application', Materials Research Society, Pittsburgh, PA, 1995, **372,** 3
2 Sargeant, G. K. *Brit. Ceram. Trans. J.* 1991, **90,** 123
3 Masters, K. 'Spray Drying Handbook', 5th edn, 1991, p. 193
4 Zhang, S. C., Messing, G. L., Lee, S. Y. and Santoro, R. J. in 'Hollow and Solid Spheres and Microspheres: Science and Technology Associated With Their Fabrication and Application', Materials Research Society, Pittsburgh, PA, 1995, **372,** 49
5 Cook, R. in 'Hollow and Solid Spheres and Microspheres: Science and Technology Associated With Their Fabrication and Application', Materials Research Society, Pittsburgh, PA, 1995, **372,** 101
6 Arshady, R. *Polym. Eng. Sci.* 1990, **30,** 915
7 Norimatsu, T., Takagi, M., Izawa, T., Nakai, S. and Yamanaka, C. *J. Vac. Sci. Technol. A* 1987, **5,** 2785.
8 Crane, R. H. *The Physics Teacher*, Dec. 1986, 561
9 Kopp, R. H. *Abrasive Engineering*, Jan/Feb 1973, 22
10 Service, R. F. *Science* 1995, **267,** 327
11 Wong, M. and Suslick, K. S. in 'Hollow and Solid Spheres and Microspheres: Science and Technology Associated With Their Fabrication and Application', Materials Research Society, Pittsburgh, PA, 1995, **372,** 89
12 Pope, E. J. A. in 'Hollow and Solid Spheres and Microspheres: Science and Technology Associated With Their Fabrication and Application', Materials Research Society, Pittsburgh, PA, 1995, **372,** 253
13 Speckman, D. M. and Jackson, C. A. in 'Hollow and Solid Spheres and Microspheres: Science and Technology Associated With Their Fabrication and Application', Materials Research Society, Pittsburgh, PA, 1995, **372,** 247
14 Craxton, R. S., McCrory, R. L. and Soures, J. M. *Sci. Amer.* 1986, **255,** 68
15 Crawley, R. *J. Vac. Sci. Technol. A* 1986, **4,** 1138
16 Kool, L. B., Nolen, R. L. and Sherwood, K. W. *J. Vac. Sci. Technol.* 1981, **18,** 1233
17 Kim, N. K., Kim, K., Payne, D. A. and Upadhye, R. S. *J. Vac. Sci. Technol. A* **7,** 1989, 1181
18 Jang, K. Y., Kim, K. and Upadhye, R. S. *J. Vac. Sci. Technol. A* 1990, **8,** 1732
19 Takagi, M., Ishihara, M., Norimatsu, T., Yamanaka, T., Izawa, Y. and Nakai, S. *J. Vac. Sci. Technol. A* 1993, **11,** 2837
20 Takagi, M., Norimatsu, T., Yamanaka, T. and Nakai, S. *J. Vac. Sci. Technol. A* 1991, **9,** 2145
21 Kubo, U. and Tsubakihara, H. *J. Vac. Sci. Technol. A* 1986, **4,** 1134
22 Calderbank, D. H. *Trans. Instn. Chem. Engrs* 1958, **36,** 443
23 Wilemski, G., Boone, T., Cheung, L., Nelson, D. and Cook, R. *Fusion Technol.* 1995, **28,** 1773